Naval Research Laboratory
Washington, DC 20375-5320

NRL/6810/MR—2022/2

Space Radiation Cover Glass Experiment Part I: Calculations

BRADLEY WEAVER

Quantum and Optoelectronics Branch
Electronics Science and Technology Division

November 2, 2022

REPORT DOCUMENTATION PAGE

Form Approved
OMB No. 0704-0188

1. REPORT DATE *(DD-MM-YYYY)*	**2. REPORT TYPE**	**3. DATES COVERED** *(From - To)*
02-11-2022	NRL Memorandum Report	10/2019 – 09/2022

4. TITLE AND SUBTITLE

Maxar-NRL Space Radiation Cover Glass Experiment - Part I: Calculations

5a. CONTRACT NUMBER

5b. GRANT NUMBER

5c. PROGRAM ELEMENT NUMBER

6. AUTHOR(S)

Bradley D. Weaver

5d. PROJECT NUMBER

5e. TASK NUMBER

5f. WORK UNIT NUMBER
1R07

7. PERFORMING ORGANIZATION NAME(S) AND ADDRESS(ES)

Naval Research Laboratory
4555 Overlook Avenue, SW
Washington, DC 20375-5320

8. PERFORMING ORGANIZATION REPORT NUMBER

NRL/6810/MR--2022/2

9. SPONSORING / MONITORING AGENCY NAME(S) AND ADDRESS(ES)

Naval Research Laboratory
4555 Overlook Avenue, SW
Washington, DC 20375-5320

10. SPONSOR / MONITOR'S ACRONYM(S)

NRL

11. SPONSOR / MONITOR'S REPORT NUMBER(S)

12. DISTRIBUTION / AVAILABILITY STATEMENT

DISTRIBUTION STATEMENT A: Approved for public release; distribution is unlimited.

13. SUPPLEMENTARY NOTES

14. ABSTRACT

As commercial satellite launches become more common and the number of trajectories available for achieving a given orbit increases, the need will also increase for a way to model the radiation exposure for such missions. By using the concepts of ionizing energy loss and the ionization damage dose, we modeled the radiation exposure of five different electric orbit raising trajectories for satellites whose ultimate mission is 15-years in geosynchronous orbit. We report on the modeling process here.

15. SUBJECT TERMS

Space radiation environment
Ionization
Displacement damage
Ionization damage electric orbit raising

16. SECURITY CLASSIFICATION OF:			**17. LIMITATION OF ABSTRACT**	**18. NUMBER OF PAGES**	**19a. NAME OF RESPONSIBLE PERSON**
					Bradley D. Weaver
a. REPORT	**b. ABSTRACT**	**c. THIS PAGE**	U	19	**19b. TELEPHONE NUMBER** *(include area code)*
U	U	U			(703) 732-4173

Standard Form 298 (Rev. 8-98)
Prescribed by ANSI Std. Z39.18

This page intentionally left blank.

SPACE RADIATION COVER GLASS EXPERIMENT
PART I: CALCULATIONS

B.D. Weaver, Naval Research Laboratory, Washington, DC, 20375

Abstract

As commercial satellite launches become more common and the number of trajectories available for achieving a given orbit increases, the need will also increase for a way to model the radiation exposure for such missions. By using the concepts of ionizing energy loss and the ionization damage dose, we modeled the radiation exposure of five different electric orbit raising trajectories for satellites whose ultimate mission is 15-years in geosynchronous orbit. We report on the modeling process here.

Introduction

Despite more than half a century of solar cell cover glass (CG) engineering, exposure to space radiation still causes CGs to darken.[1,2] Darkening reduces the amount of light that reaches the underlying solar cells and decreases their photoconversion efficiency. In an effort to better understand radiation-induced cover glass darkening, Maxar engaged the U.S. Naval Research Laboratory (NRL) to perform modeling, simulations, and ground-based radiation tests using Qioptiq CMG cover glass materials intended to protect solar power cells during low-thrust electric orbit raising (EOR) transfer orbits from low earth orbit (LEO) to geostationary orbit (GEO), and for a 15 year mission in GEO.

The results of this investigation are presented in three reports. First, in this report, a foundation is established for designing a ground-based experiment for testing the responses of various CGs to selected EOR+GEO missions. The following topics are covered:

- The space radiation environment and radiation effects;
- Qioptiq CMG cover glass overview;
- Electric orbit raising; five Maxar trajectories;
- Discreet versus continuous radiation spectra
- Simulations and calculations: Determining the ionizing energy loss (IEL)
- Ionization damage dose (IDD)
- IDD, and five complete missions
- Reverse engineering and ground test basics
- Summary and conclusions

The experimental design and radiation test plan will be described in the second report, and the results, analysis and discussion will be presented in the third.

Manuscript approved October 26, 2022.

Space Radiation Environment and Radiation Effects

There are three main sources of radiation damage in space: Earth's Van Allen belts, the solar wind, and cosmic rays. The Van Allen belts are zones of energetic particles captured by Earth's magnetic field. The inner belt consists mainly of protons, and ranges from about 600 km above the surface to about 10,000 km, although the distance can vary depending on solar activity. The outer electron belt ranges from about13,500 km to about 58,000 km above the surface. The solar wind is a stream of charged particles released from the sun's corona, and consists mainly of electrons, protons, and alpha particles, although trace amounts of other elements such as carbon, nitrogen, and neon are also present. Cosmic rays are high-energy protons and bare atomic nuclei, mostly of extrasolar origin. About 90% of cosmic rays are protons, 9% are helium nuclei, and 1% are heavier nuclei.

Radiation damage can take any of three forms. These are displacement damage, which causes atoms to be displaced from their initial lattice sites; ionization damage, which results in trapped charge; and single event effects (SEEs) such as latch-ups, bit-flips and burnout. (SEEs are not relevant to CGs so are not considered here.) Ionization damage is more readily produced than displacement damage because less energy is required to move an electron than an atom. The parameter of note for quantifying ionization effects is the ionizing energy loss (IEL), which is defined as the density-normalized rate at which an incident particle loses energy to ionization within a material. Its units are MeV•cm^2/g. However, it must be noted that IEL is also commonly expressed in a non-density-normalized form, and has units eV/Å•ion. Nonionizing energy loss (NIEL) is the density-normalized rate at which an incident particle loses energy to producing displacements. In many cases NIEL and IEL are directly proportional, but in some cases – particularly for lower energy, lighter particles such as electrons in the keV range – they can be much different.

Two additional parameters based on IEL and NIEL are commonly used when discussing ionizing and nonionizing radiation damage effects. These are the ionization damage dose, IDD, and the displacement damage dose, DDD. Both are directly proportional to the concentration of induced defects, whether ionized or nonionized. The IDD is given by

$$IDD = IEL \bullet \phi \ , \qquad (1)$$

where ϕ is the fluence of incident particles (particles/cm^2). Similarly, DDD is the product of NIEL and ϕ.

In solar cell cover glasses, the dominant radiation effect is due to ionization. When an incident energetic particle encounters an insulating material such as a CG, it immediately begins to transfer energy to its environment, in part by exciting carriers into the conduction band. The surge of carriers causes the insulator to become locally conductive. The particle passes, and the deposited energy dissipates. In the short time it takes for the insulating state to return, most excited carriers are able to recombine, but a few remain behind as trapped charge. Trapped charge introduces defect levels in the local band structure, which allow photons of specific wavelengths to be absorbed. These defects are called color centers. Light absorbed by color centers in CGs doesn't reach the solar cell, and so can't contribute to the power generation that drives the EOR process.

The wavelengths of light absorbed by color centers depend on the type, location and nature of the trapped charge, and can vary widely. The visible result is often a yellowing or browning of the glass. The variety of color centers that can be produced depends on the properties of the CG itself, and not on any characteristic of the incident particle. The density of color centers produced, however, depends entirely on the incident particle mass, energy, and the fluence ϕ to which the samples are exposed. Hence, the quality of color centers depends on the CG, but the quantity depends on the space radiation environment by way of the ionization damage dose IDD.

Qioptiq CMG Cover Glass Overview

Qioptiq CMG cover glass is used in this experiment. The composition is primarily SiO_2, but the glass contains fourteen different additives that act to mitigate radiation-induced color centers. The proprietary additives include elements and chemical compounds in atomic fractions ranging from 0.5% to 5%.

Two cover glass thicknesses are used: 100 µm and 125 µm. In addition, half each of the two thicknesses of CGs have a 0.145 µm-thick MgF_2 antireflective (AR) coating, while the other half do not. Each cover glass measures 1 cm x 1 cm. Before irradiation, the transmission properties of all CGs were characterized at Qioptiq and again at NRL. Following the preliminary characterization, ground-based irradiation experiments were performed to simulate space radiation exposure for the five missions. The optical characteristics of the CGs was then re-measured to quantify the amount of darkening. Details of this procedure are given in Parts 2 and 3 of this series.

Electric Orbit Raising; Five Maxar Trajectories

Launching a satellite directly into geosynchronous orbit is expensive. Enabling it to raise its own orbit by means of solar electric propulsion and launching the satellite into LEO instead is more cost-effective.[3] The trade-off for doing so is that in order to reach GEO from LEO, the satellite must traverse Earth's Van Allen belts. A sample EOR trajectory is shown in Fig. 1. As can be seen, the satellite crosses the inner and outer belts many times before settling into GEO.

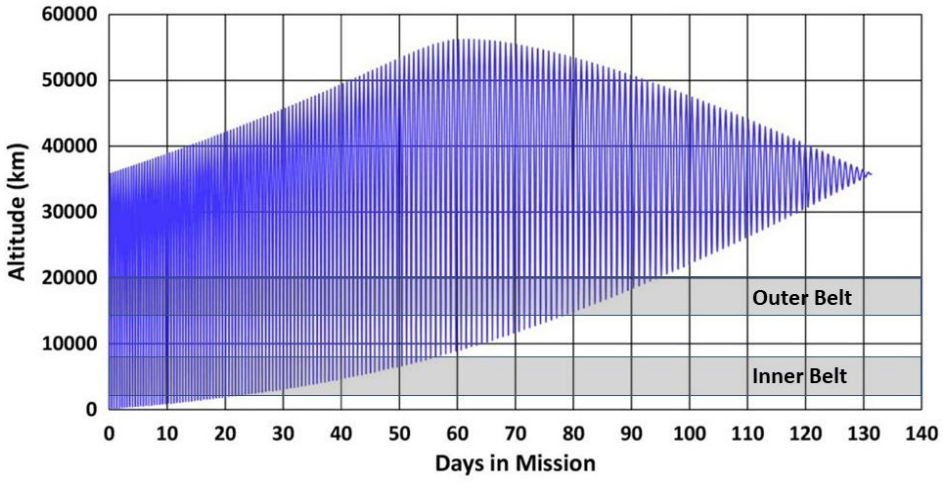

Fig. 1. Schematic EOR trajectory from LEO to GEO. The hearts of the inner and outer Van Allen belts are shown. The satellite traverses the belts many times before reaching GEO. (Modified from ref. 4.)

All components of the spacecraft, including CGs, must be able to withstand this transition. For the Maxar-NRL cover glass experiment, five EOR radiation scenarios have been selected. These are called Ariane 190, Ariane GTO, Ariane SSTO, Falcon-9, and Maxar Worst-Case (WC). Fluences of electrons and protons for the various EOR trajectories are listed in Tables 1 and 2. Energies at which implantation into the CG occurs are shaded in gray.

Energy (MeV)	Ariane-190 $\phi(e^-/cm^2)$	Ariane GTO $\phi(e^-/cm^2)$	Ariane SSTO $\phi(e^-/cm^2)$	Falcon-9 $\phi(e^-/cm^2)$	Maxar WC $\phi(e^-/cm^2)$
0.04	6.82E15	2.70E15	1.43E15	2.55E15	1.22E15
0.07	4.23E15	1.54E15	8.07E14	1.39E15	
0.10	2.60E15	1.00E15	5.03E14	8.77E14	7.95E14
0.25	6.28E14	3.55E14	1.43E14	2.82E14	
0.50	2.28E14	1.16E14	4.86E13	8.94E13	9.99E13
0.75	1.16E14	5.85E13	2.35E13	4.41E13	
1.00	6.57E13	3.41E13	1.31E13	2.55E13	2.67E13
1.50	2.24E13	1.13E13	4.54E12	8.11E12	
2.00	7.73E12	3.41E12	1.60E12	2.50E12	3.86E12
2.50	2.86E12	1.25E12	5.55E11	9.16E11	1.55E12
3.00	1.11E12	5.21E11	2.25E11	3.84E11	5.87E11
3.50	4.77E11	2.29E11	1.00E11	1.67E11	2.15E11
4.00	2.24E11	1.04E11	4.66E10	7.52E10	6.7E10
4.50	1.13E11	5.02E10	2.34E10	3.61E10	1.82E10
5.00	5.98E10	2.75E10	1.37E10	1.95E10	4.02E9
5.50	3.36E10	1.76E10	9.33E9	1.24E10	
6.00	2.01E10	1.24E10	6.88E9	8.64E9	
6.50	1.26E10	9.00E9	5.19E9	6.23E9	
7.00	8.34E9	6.71E9	3.94E9	4.63E9	
7.50	5.85E9	5.08E9	3.00E9	3.50E9	
8.00	3.92E9	3.69E9	2.19E9	2.55E9	

Table 1. Electron fluences for five EOR trajectories. Shaded rows indicate e^- implantation.

Energy (MeV)	Ariane-190 $\phi(p^+/cm^2)$	Ariane GTO $\phi(p^+/cm^2)$	Ariane SSTO $\phi(p^+/cm^2)$	Falcon-9 $\phi(p^+/cm^2)$	Maxar WC $\phi(p^+/cm^2)$
0.1	5.39E14	5.98E14	2.01E14	4.37E14	8.70E14
0.2	3.52E14	3.24E14	9.99E13	2.37E14	
0.5	1.24E13	9.10E13	2.02E13	6.52E13	1.67E14
0.6	9.66E13	6.53E13	1.26E13	4.65E13	
0.8	4.77E13	3.55E13	5.50E12	2.46E13	
1.0	3.00E13	2.14E13	2.66E12	1.45E13	4.13E13
3.0	3.56E12	1.78E12	6.63E10	1.16E12	2.21E12
4.0	1.22E11	6.30E11	7.28E9	4.09E11	1.03E12
6.0	2.65E11	1.73E11	7.50E8	1.19E11	
8.0	8.56E10	6.01E10	1.54E8	4.97E10	
10	4.17E10	3.28E10	7.50E7	3.01E10	1.09E11
15	1.41E10	1.32E10	2.78E7	1.51E10	
20	8.45E9	8.19E9	1.52E7	1.02E10	
30	6.21E9	5.30E9	7.97E6	6.77E9	8.50E9
50	4.78E9	3.04E9	3.23E6	4.00E9	
60	4.34E9	2.40E9	2.15E6	3.28E9	4.06E9
80	3.69E9	1.68E9	9.63E5	2.39E9	
100	3.14E9	1.21E9	4.44E5	1.78E9	2.31E9
150	2.09E9	5.45E8	1.15E5	9.03E8	
200	1.32E9	2.43E8	3.12E4	4.77E8	
250	8.15E8	1.23E8	1.05E4	2.65E8	

Table 2. Proton fluences for five EOR trajectories. Shaded rows indicate p^+ implantation.

In addition to radiation exposure during the EOR transfers, satellites encounter a radiation environment at GEO. Fluences are given in Table 3 for electrons, and Table 4 for protons and alphas. (Alpha fluences during EOR are negligible.)

Electron Energy (MeV)	Typical GEO 15 year fluence (e^-/cm^2)	Maxar WC 15 year fluence (e^-/cm^2)
0.04	1.89E16	2.19E16
0.10	1.24E16	1.51E16
0.25	4.10E15	5.30E15
0.50	1.03E15	1.40E15
0.75	3.51E14	5.58E14
1.00	1.54E14	2.34E14
1.50	3.65E13	5.87E12
2.00	1.12E13	1.96E13
2.50	2.75E12	5.16E11
3.0	1.02E12	1.83E12
3.5	4.26E11	7.57E10
4.0	4.23E11	2.15E11
4.5	3.76E10	5.63E10
5.0	1.05E9	2.14E9

Table 3. Fifteen year electron fluences in GEO for typical and Maxar WC scenarios. Shaded rows indicate electron implantation in the CG.

Energy E (MeV)	Proton Fluence (p^+/cm^2)	Alpha Fluence (α/cm^2)	Proton Range (μm)	Alpha Range (μm)
0.01	1.36E16	---	0.11	
0.03	1.01E16	---	0.26	
0.05	7.5E15	---	0.38	
0.10	3.16E15	---	0.66	
0.50	5.2E13	---	4.01	
1.00	1.4E12	7.00E10	11.0	2.49
4.00	2.5E11	1.24E10	99.4	11.7
10.00	1.1E11	5.49E9	481	46.2
30.00	4.00E10	2.01E9	3390	292
60.00	1.26E10	6.29E8	11730	987
100.00	2.80E9	1.41E8	29100	2450

Table 4. Proton and alpha fluences for a 15 year GEO mission. Shaded cells indicate implantation. Proton and alpha ranges in the CGs are also listed for reference. The same fluences are used for the Maxar WC mission.

Discrete Versus Continuous Radiation Spectra

The data of Tables 1 – 4 show fluences falling into discrete energy bands, which is how the data are collected in space. Radiation detectors have separate 'bins' that count particles whose energy lies within a specific range. The true space radiation environment has a full and continuous energy spectrum. Two approaches are commonly used to address this compartmentalization effect. The first is to accept the stepwise data as being representative of the true space radiation environment. The second is to use interpolative software to approximate a continuous spectrum from the discrete data. A modified version of the discrete approach is used here. The data of Tables 1 and 3 for electrons in the implantation range of energies have been broken into smaller bands, using the assumption that the fluence of particles is uniform across each band. Results are shown in Tables 5 and 6.

Energy (MeV)	Ariane-190 $\phi(e^-/cm^2)$	Ariane GTO $\phi(e^-/cm^2)$	Ariane SSTO $\phi(e^-/cm^2)$	Falcon-9 $\phi(e^-/cm^2)$	Maxar WC $\phi(e^-/cm^2)$
0.010	9.70E+14	3.90E+14	2.00E+14	3.60E+14	1.70E+14
0.015	9.7E+14	3.9E+14	2.00E+14	3.6E+14	1.70E+14
0.020	9.7E+14	3.9E+14	2.00E+14	3.6E+14	1.70E+14
0.025	9.7E+14	3.9E+14	2.00E+14	3.6E+14	1.70E+14
0.030	9.7E+14	3.9E+14	2.00E+14	3.6E+14	1.70E+14
0.035	9.7E+14	3.9E+14	2.00E+14	3.6E+14	1.70E+14
0.040	9.7E+14	3.9E+14	2.00E+14	3.6E+14	1.70E+14
0.045	1.06E+15	3.85E+14	2.02E+14	3.48E+14	1.13E+14
0.05	1.06E+15	3.85E+14	2.02E+14	3.48E+14	1.13E+14
0.06	1.06E+15	3.85E+14	2.02E+14	3.48E+14	1.13E+14
0.07	1.06E+15	3.85E+14	2.02E+14	3.48E+14	1.13E+14
0.08	8.70E+14	3.30E+14	1.68E+14	2.92E+14	1.13E+14
0.09	8.70E+14	3.30E+14	1.68E+14	2.92E+14	1.13E+14
0.10	8.70E+14	3.30E+14	1.68E+14	2.92E+14	1.13E+14
0.15	2.09E+14	1.18E+14	4.80E+13	9.40E+13	3.33E+13
0.20	2.09E+14	1.18E+14	4.80E+13	9.40E+13	3.33E+13
0.25	2.09E+14	1.18E+14	4.80E+13	9.40E+13	3.33E+13

Table 5. Enhanced data for replacing the first four rows of Table 1.

Energy (MeV)	GEO e^- Normal $\varphi(e^-/cm^2)$	GEO Worst-Case $\varphi(e^-/cm^2)$
0.010	2.75E+15	3.13E+15
0.015	2.75E+15	3.13E+15
0.020	2.75E+15	3.13E+15
0.025	2.75E+15	3.13E+15
0.030	2.75E+15	3.13E+15
0.035	2.75E+15	3.13E+15
0.040	2.75E+15	3.13E+15
0.045	1.77E+15	2.16E+15
0.050	1.77E+15	2.16E+15
0.060	1.77E+15	2.16E+15
0.070	1.77E+15	2.16E+15
0.080	1.77E+15	2.16E+15
0.090	1.77E+15	2.16E+15
0.100	1.77E+15	2.16E+15
0.150	1.77E+15	1.37E+15
0.200	1.77E+15	1.37E+15
0.250	1.77E+15	1.37E+15

Table 6. Expanded data for replacing the first three rows of Table 3.

Simulations and Calculations: Determining the Ionizing Energy Loss (IEL)

Now that the space radiation environments have been specified, the associated values for the ionizing energy loss must be calculated. IEL values for protons and alpha particles were determined using the Monte Carlo program SRIM.[5] Required inputs for SRIM are the chemical and physical composition of the target material, including the density, the displacement energy thresholds for each type of atom, the atomic percentages of each element, and the target thickness. The displacement energy threshold E_d is the minimum energy required to displace an atom from its initial position. Values of E_d ranged upward from 20 eV for oxygen atoms in the SiO_2, and were either determined from the literature or inferred from existing data.[6-13] The simulation program mathematically divides each cover glass into 100 planar slices of thickness 1.00 µm or 1.25 µm, depending on the original CG thickness (100- or 125 µm), before performing a detailed calculation of defect formation, including full damage cascades.

Values of IEL for electrons were extracted from the National Institute of Standards and Technology's ESTAR data, and supporting information was obtained by using the program SR-NIEL.[14,15] The ESTAR units for IEL are MeV•cm^2/g, while units for IEL produced by SRIM and SR-NIEL are eV/Å•ion. For Qioptiq CMG cover glass, data having units MeV•cm^2/g can be converted to eV/Å•ion by multiplying the MeV•cm^2/g data by 0.316.

Simulations were performed on the AR coating alone with no CG beneath it to determine whether its presence affected the overall results. Considering that its thickness is only 0.145 µm, which is at most 0.145% of the total CG thickness, it is not surprising that no noticeable effect was observed. Hence for the remainder of the discussion on IEL the AR coating will be neglected.

Results of the calculations are summarized in Table 7. Electrons having energies less than about 0.10 MeV are always implanted regardless of CG thickness or whether an AR coating is present. For protons having E ≥ 50 MeV, and for alphas having E ≥ 100 MeV, the particles traverse the CG without significant loss of energy. For proton energies between 50 MeV and 4.5 MeV, and for alpha energies down to 15 MeV, the particles lose a noticeable amount of energy before exiting the CG. This energy loss is indicated in Table 7 by two numbers: The IEL of the particle as it enters and as it exits the CG. For example, a 6 MeV proton enters with IEL = 1.65 eV/Å•ion and leaves with IEL = 2.43 eV/Å•ion. The corresponding entry in Table 7 is 1.65-2.43. As another example, the initial value for 10 MeV alphas is 13 eV/Å•ion. It then reaches a maximum of 48 eV/Å•ion, after which it quickly falls to 0 as the ion implants. The corresponding entry is 13-48-0.

The ionizing energy loss as a function of distance into a CG is shown in Fig. 2 for 1 MeV-, 4 MeV-, and 8 MeV protons. The 1- and 4 MeV protons undergo implantation. The IEL for the 1 MeV proton is initially 5.7 eV/Å•ion, reaches a maximum at 13.5 eV/Å•ion and then falls to 0. The entry for 1 MeV protons in Table 7 is 5.7-13.5-0.

As a further example, IEL curves for alpha particles are shown in Fig. 3 as a function of distance into the CG.

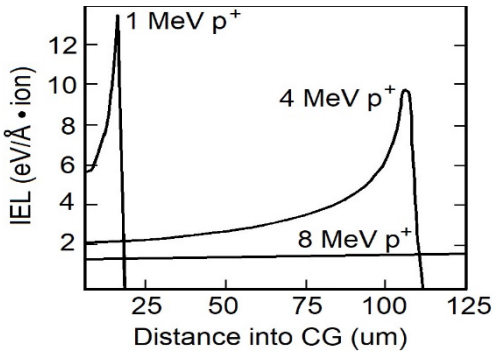

Fig. 2. IEL for protons of various energies as a function of distance into a Qioptiq CMG CG. All implantation profiles are called 'Bragg curves'.

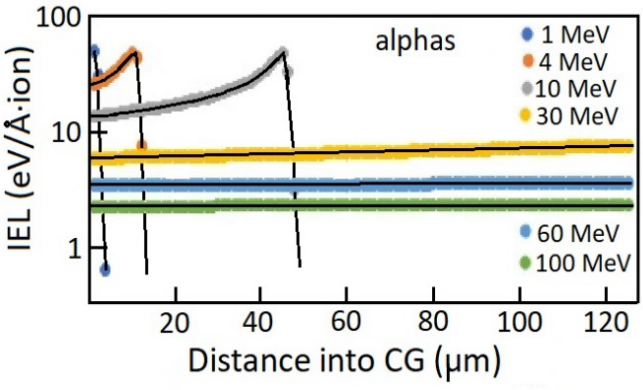

Fig. 3. IEL for alpha particles vs distance into CG for a 15 year GEO mission.

Energy (MeV)	Electron IEL (eV/Å•ion)	Electron Range (µm)	Proton IEL (eV/Å•ion)	Proton Range (µm)	Alpha IEL (eV/Å•ion)	Alpha Range (µm)
0.01			8.9	0.11		
0.03			8.9	0.26		
0.04	1.98	21.2				
0.05			8.9	0.38		
0.07	1.34	42.5				
0.10	1.06	63.8	8.9	0.66		
0.20			8.9	1.28		
0.25	0.66	255				
0.50	0.53	765	8.9	4.01		
0.60			7.8-13.7-0	5.18		
0.75	0.50	1110				
0.80			6.5-12.3-0	7.87		
1.00	0.49	1700	5.7-13.5-0	11.0	48	2.49
1.50	0.49	3150				
2.00	0.49	4000				
2.50	0.51	4300				
3.00	0.52	5950	2.8-10.5-0	61.6		
3.50	0.52	7050				
4.00	0.53	8500	2.2-9.7-0	99.4	25-48-0	11.7
4.50	0.54	9350				
5.00	0.55	10200				
5.50	0.55	10600				
6.00	0.56	11000	1.65-2.43	198		
6.50	0.57	11900				
7.00	0.58	12800				
7.50	0.58	13600				
8.00	0.59	14500	1.32-1.61	326		
10.0			1.11-1.26	482	13-48-0	46.2
15.0			0.81-0.86	985		
20.0			0.65-0.67	1640		
30.0			0.48-0.49	3390	5.9-7.6	292
50.0			0.31	8460		
60.0			0.27	11700	3.4-3.6	987
80.0			0.22	19600		
100			0.19	29100	2.3	2450
150			0.14	59300		
200			0.12	97400		
250			0.10	142000		

Table 7. Ionizing energy loss for electrons, protons and alpha particles in 125 µm-thick Qioptiq CMG cover glass. Shaded cells indicate particle implantation.

Ionization Damage Dose

Example 1: Geosynchronous Orbit. To convert the IEL data for alphas in Fig. 3, for example, to IDD, Eq. (1) is used in conjunction with the alpha fluence data of Table 4 and the IEL data of Table 7. Results are shown in Fig. 4, where IDD is plotted as a function of distance into the CG. The initial units, (eV/Å•ion) x (ion/cm^2), have been converted to the more convenient units MeV/g. Keep in mind that the IDD is directly proportional to the induced color center density, and hence to the degree of CG darkening. The stepwise appearance of the "Total" curve is due to the discrete particle energy spectrum used.

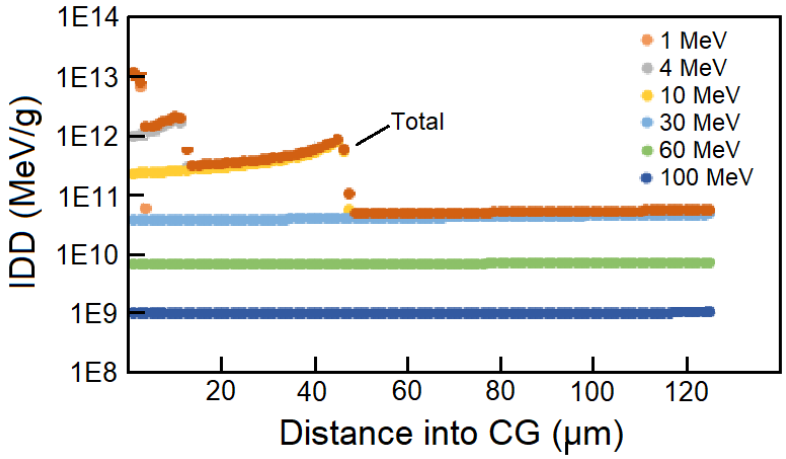

Fig. 4. Ionization damage dose vs depth into CG for various alpha particles over a 15 year GEO mission.

Determining the total IDD for protons over a 15 year GEO mission follows a similar process, using IEL data from Table 7, fluence data from Table 4, and Eq. (1). Results are shown in Fig. 5. Note the vestiges of Bragg curves in Figs. 4 and 5. This is also an indication of discrete spectra being used.

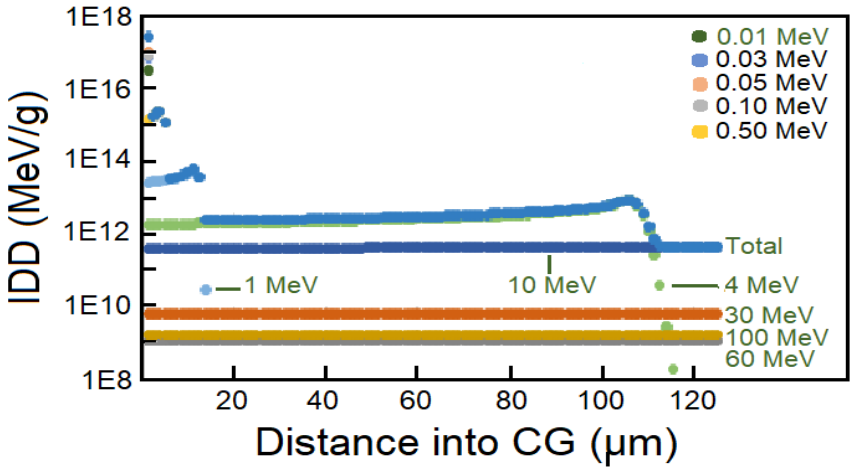

Fig. 5. Ionization damage dose versus depth into a CG for various proton energies over a 15 year GEO mission.

Figure 6 shows IDD curves for GEO mission electrons, including the normal and worst-case scenarios of Table 3. The enhanced electron spectrum of Table 6 has been used for Fig. 6. The 'worst-case' scenario produces more damage near the front of the CG, but less damage near the rear.

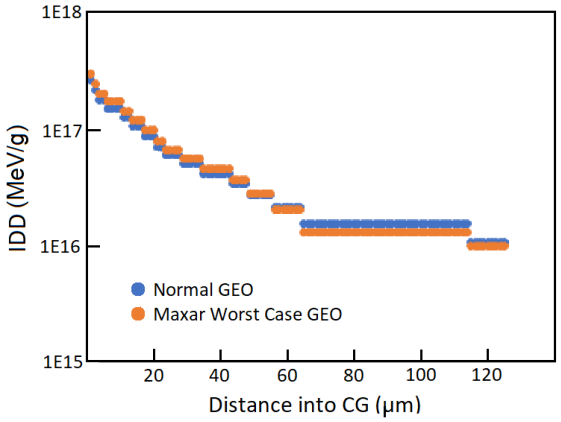

Fig. 6. Ionization damage dose versus depth into CG for a 15 year GEO mission. The expanded data set for GEO electrons from Table 6 has been used.

The total ionization damage dose for electrons, protons and alpha particles for the two GEO mission scenarios is plotted in Fig. 7. The inset of Fig. 7 shows the relative contributions of alpha particles (blue), protons (orange) and electrons (green) to the total GEO radiation environment. The GEO orbit is clearly dominated by electron damage.

Ionization Damage Dose, Example 2: The EOR trajectories. The ionization damage dose for electrons is shown in Fig. 8 for each of the EOR trajectories.

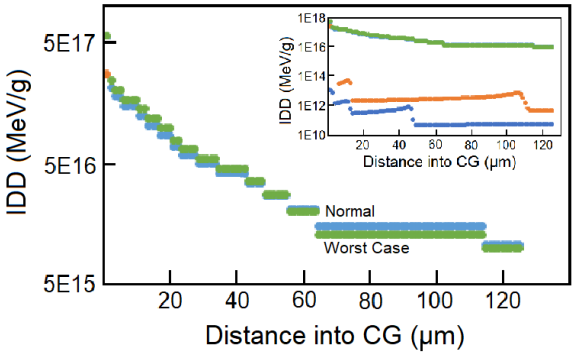

Fig. 7. Total IDD vs depth into a CG for normal and worst-case GEO missions. Inset: Relative contribution of protons (red), alphas (blue) and electrons (green).

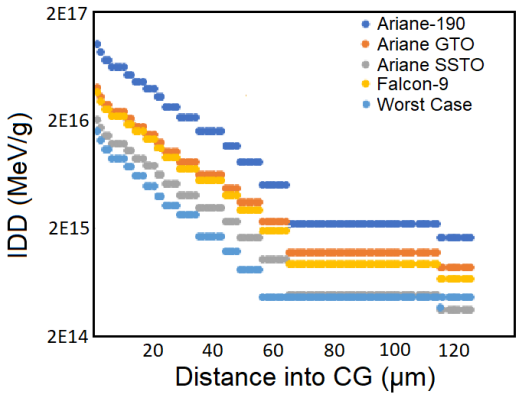

Fig. 8. IDD for EOR electrons. Data from the expanded electron set were used.

The most radiation damage occurs for the Ariane 190 day EOR trajectory, followed by the Ariane GTO, Falcon-9, Ariane SSTO, and the Worst-Case. For EOR protons, shown in Fig. 9, the radiation exposure is very similar for four of the trajectories but significantly lower for the Ariane SSTO path.

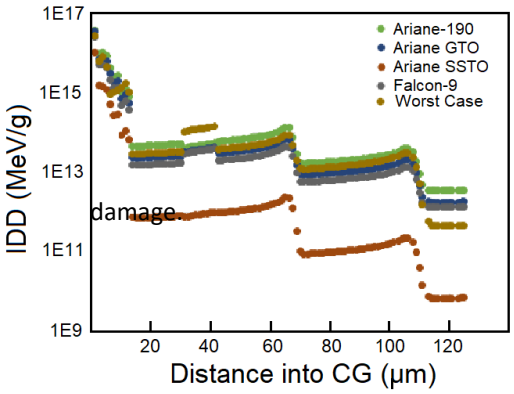

Fig. 9. IDD for EOR protons vs distance into CG. The Ariane SSTO trajectory experiences the least

Using the ionization damage dose allows the electron data of Fig. 8 to be added directly to the proton data of Fig. 9. (Recall that EOR trajectories do not include alpha particles). Results are shown in Fig. 10.

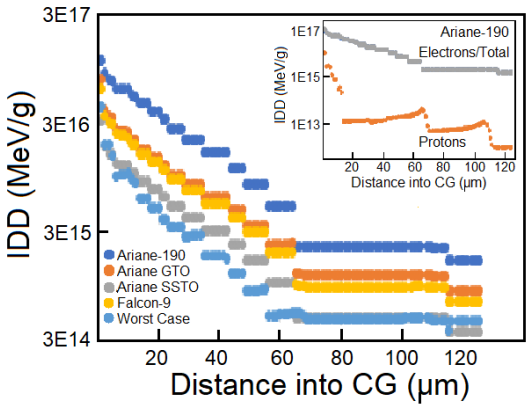

Fig. 10. Total IDD for all EOR trajectories. Inset: Proton and electron damage for the Ariane-190 day EOR trajectory for comparison.

Ionization Damage Dose, Example 3: Five Complete Missions. During the EOR phase, the radiation is harsh but the duration is relatively short. GEO radiation is less harsh but lasts for 15 years. Figures 11a-e show the total IDD for each of the five missions. The same vertical scale is used in all figures.

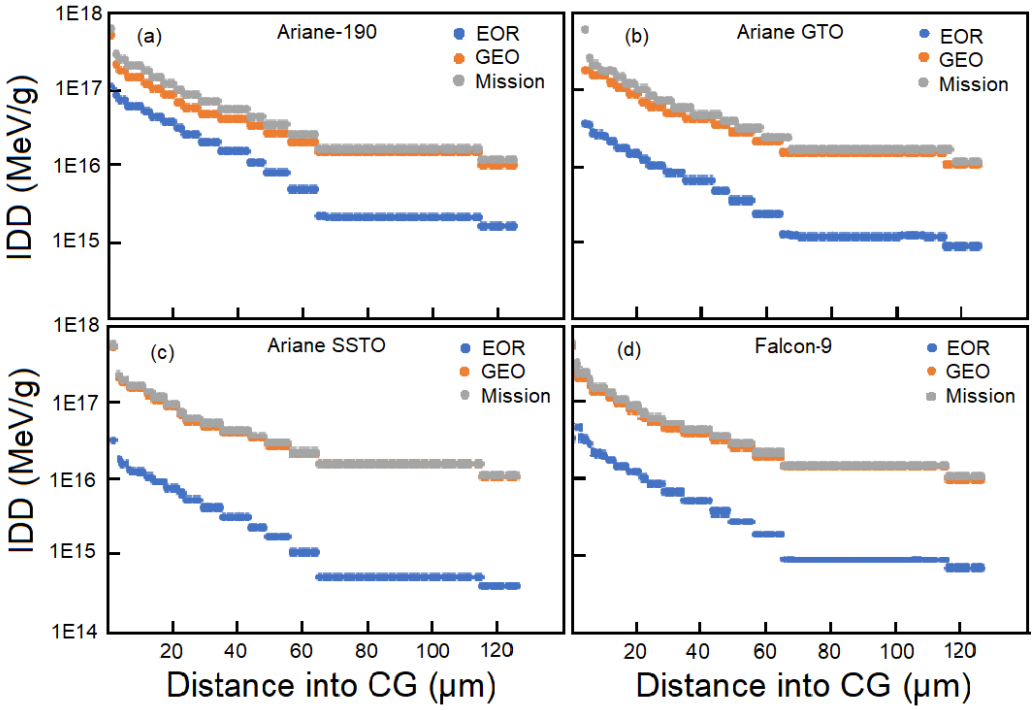

Figure 11. IDD vs distance into CG for (a) Ariane 190, (b) Ariane GTO, (c) Arians SSTO, and (d) Falcon-9 missions.

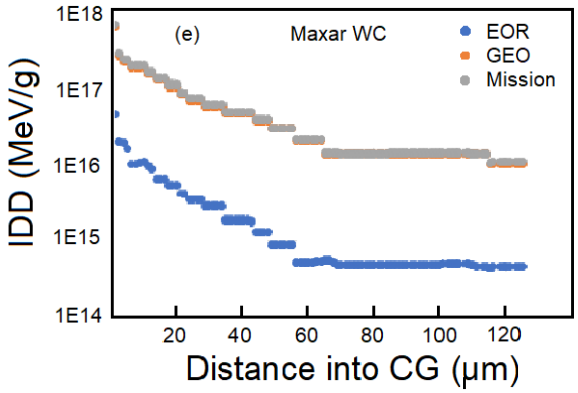

Fig. 11e. IDD vs distance into CG for Worst-Case mission.

Values of IDD for all five missions are shown versus distance into the CG in Fig. 12. Comparing Figs. 10 and 12 reveals a surprising result: Even though the ontensity of individual EOR radiation environments vary by a factor of 6, adding a 15 year mission in GEO washes out that difference. Even so, these are the curves that must be reverse-engineered to determine the ground-based irradiation protocol.

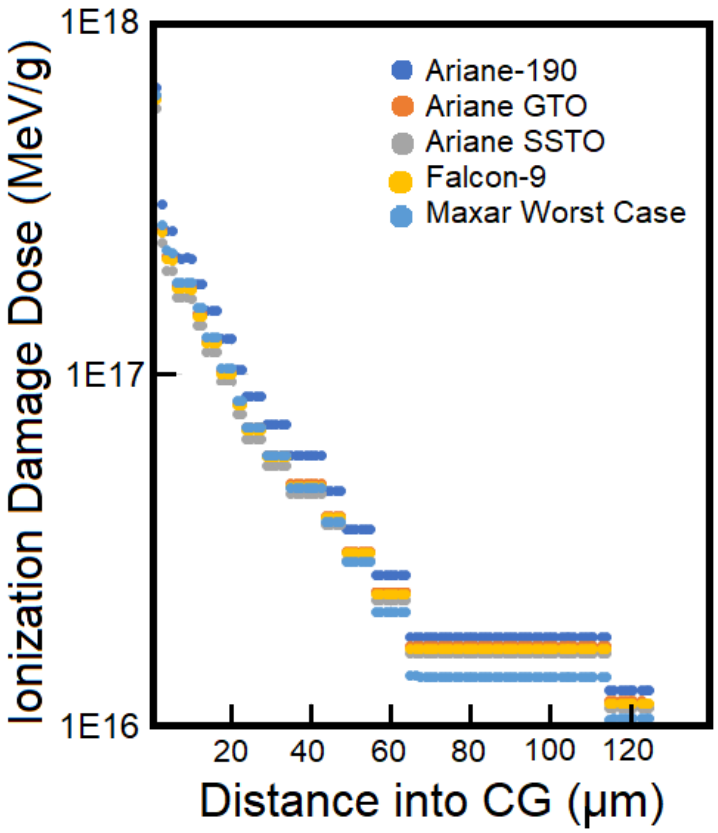

Fig. 12. IDD vs distance into a cover glass for five complete EOR+GEO missions. IDD is directly proportional to the cover glass darkening. For the Maxar WC mission, a worst-case electron spectrum was used for GEO. The radiation exposure from the GEO portion of the missions dominates the overall response.

Reverse Engineering and Ground Test Basics

There are three main approaches to ground testing CGs for space radiation hardness. The first, earliest method required only 30 keV protons incident on the top 0.26 μm of the cover glass. Using this approach allows the correct number of defects to be produced but lacks any semblance of spatial precision. The second method produced accurate defect densities *and* spatial distribution, but required up to 6 electron- and 5 proton energies, which makes it time consuming and expensive.[16,17] The third method used a combination of irradiation from the front and back of the cover glass to produce a precise damage profile with only 3 proton energies.[18] The disadvantage of this approach is that for CG thicknesses greater than about 50 μm proton energies are required that exceed those available from commercial Van de Graaff accelerators.

The CGs used in the present experiment (100- and 125 μm) are too thick to use the front-back irradiation approach of method 3 above, so a hybrid approach must be taken. Combining methods 2 and 3, a thorough damage profile can be produced with one 3.8 MeV proton irradiation through the back of the cover glass and a number of proton energies from the front. This approach is still tedious, but no electron irradiations are required, and only one radiation facility is required.

None of the above methods are sufficiently precise that damage-depth profiles can be designed to differentiate between, say, the Ariane GTO and Ariane SSTO missions (at least not without extreme cost). So understanding that, an irradiation protocol was designed, and is discussed below.

The goal of the reverse engineering process is to reproduce the same damage-depth profile on the ground as is expected in space (see Fig. 12). The first step is shown in Fig. 13(a), where the IDD curve of $4.8x10^{14}$ 3.8 MeV p^+/cm^2 incident on the back side of a 125 µm CG is shown as the the orange Bragg curve. Two additional proton fluences incident on the front of a CG ($4.1x10^{14}$ 2.25 MeV p^+/cm^2 and $1x10^{14}$ 2 MeV p^+/cm^2), the red damage curve of Fig. 13(b) results.

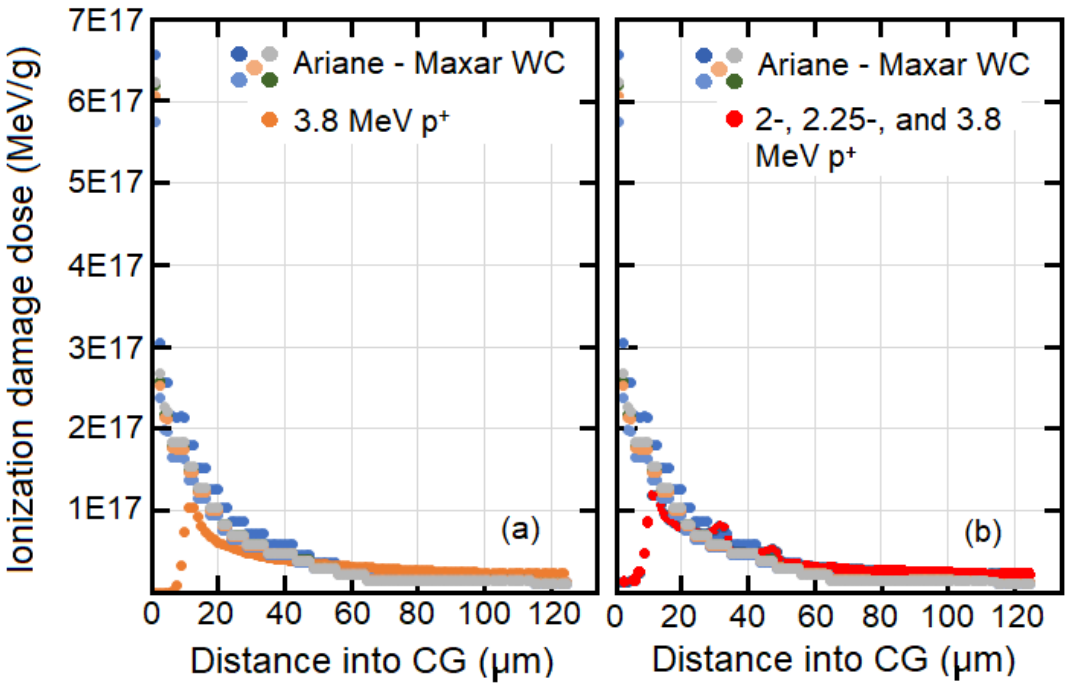

Fig. 13. Ionization damage dose vs distance into cover glass for the Ariane 190 to Maxar WC missions, and for (a) $4.8x10^{14}$ 3.8 MeV p^+/cm^2 (orange circles) incident from the back, and (b) adding $4.1x10^{14}$ 2.25 MeV p^+/cm^2, and $1x10^{14}$ 2 MeV p^+/cm^2 incident from the front of the CG. The ionization damage accumulated during fifteen years in geosynchronous orbit tends to mask the individual IDD profiles of the various EOR trajectories. Due to the front-back approach the radiation protocol can be the same for both CG thicknesses.

Continuing beyond Fig. 13 by adding more proton irradiations from the front of the CG builds a damage profile very close to the one in space. There are many possible combinations. One of them is shown in Table 8, with the accompanying damage profiles shown in red in Fig. 14. The result is very close to the damage profile expected in space.

Energy (MeV)	Fluence (p^+/cm^2)
3.80	4.8E14 back side
2.25	4.1E14 front side
2.00	1.0E14 "
1.75	1.0E14 "
1.50	1.5E14 "
0.75	3.0E15 "
0.60	2.5E15 "
0.50	1.4E15 "

Table 8. Proton irradiation protocol that produces the "Ground Test" damage profile (in red) in Fig. 14.for all CGs.

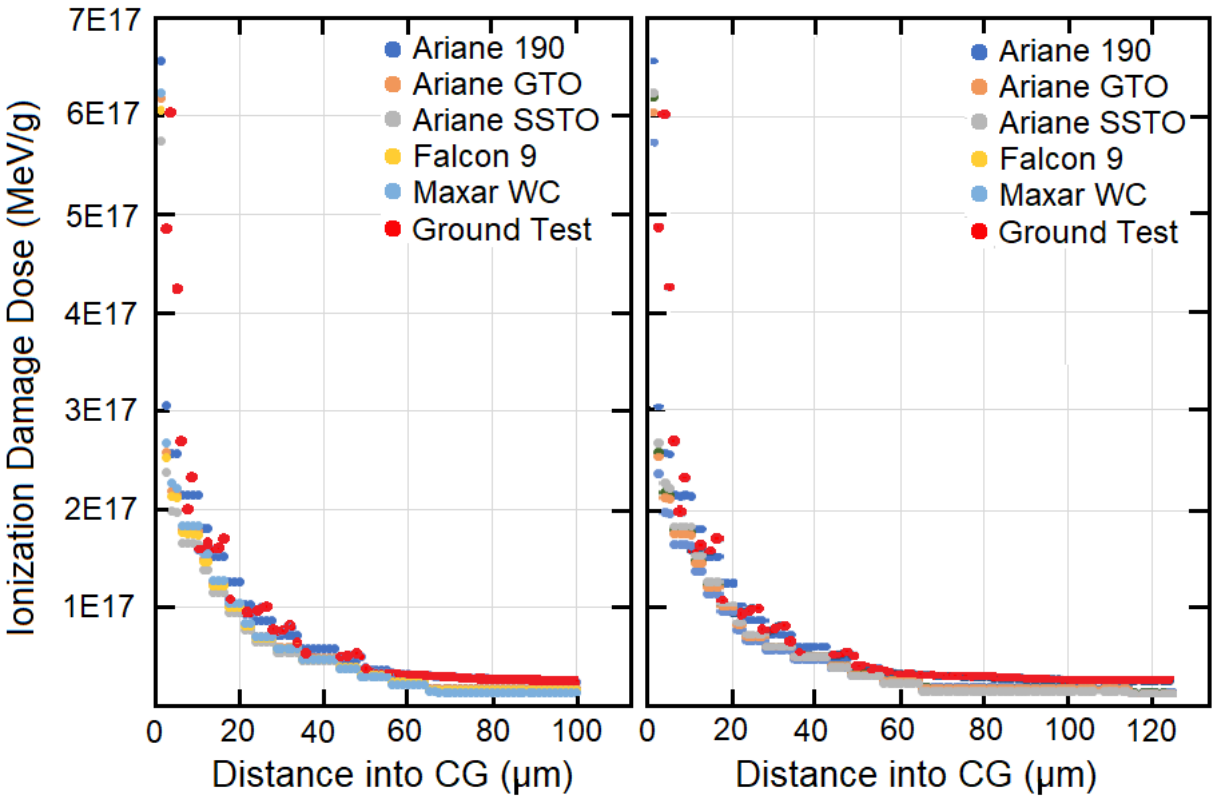

Fig. 14. IDD vs distance into CG for 100- and 125 μm thick CGs, comparing the the Ariane 190 through Maxar WC missions with the calculated depth profile created by proton irradiation. Although the initial intention was to test each mission separately, their radiation profiles are not sufficiently different that ground-based testing can differentiate between them without incurring excessive cost.

Summary and Conclusion

A process for developing ground-based tests of space radiation effects in coverglass materials is described. Seven examples are given, including five electric orbit raising trajectories and two missions in geosynchronous orbit. Developing the tests involves knowing the particular space radiation environment, the corresponding ionization damage dose, and the damage-depth profile across the coverglass.

The total dose accumulated during the EOR part of a mission depends on the trajectory, but varies by a factor of only about four between the five paths selected. The damage accumulated during 15 years in GEO is much larger in comparison and tends to minimize the differences in EOR paths. This result is a bit surprising because EOR trajectories traverse Earth's inner and outer Van Allen belts many times (up to about 90) before reaching GEO altitudes. The final ground test devised is a hybrid of the reverse-face irradiation approach of ref. 18 and the multiple energy/fluence approach of refs. 16 and 17.

The ground test procedure and the results of the experiment are forthcoming.

References

1. "Solar Cell Cover Glass Development," Quarterly Report prepared by Ion Physics Corporation, Burlington, MA for Goddard Space Flight Center, Greenbelt, MD, 1966.
2. "Effect of Radiation on Cerium-Doped Solar-Cell Cover Glass," G.A. Haynes, NASA Tech. Note TN D-6024, 1970.
3. **Fundamentals of Electric Propulsion: Ion and Hall Thrusters**, D.M. Goebel and I. Katz (Wiley, Hoboken, NJ) 2008.
4. C.A. Kluever and S.R. Oleson, "Direct approach for computing near-optimal low-thrust earth-orbit transfers," J. Spacecraft Rockets, **35**(4), 509 (1998).
5. "Stopping and Range of Ions in Matter," website: https://srim.org.
6. B.S. Thomas, N. Marks, L.R. Corrales, and R. Devanathan, Nucl. Instrum. Meth. Phys. Res. B **239**(3), 191 (2005).
7. E. Gonzales, A. Abreu, C.M. Cruz, I. Pinerd, and A. Leyva, Nucl. Instrum. Meth. Phys. Res. B **258**, 142 (2015).
8. Y.G. Yuan, M. Jiang, F.A. Zhao, H. Chen, H.Y. Xiao, X. Xiang, and X.T. Zu, Scientific Repts. **7**, 3621 (2017).
9. H. Tsuchihira, T. Oda, and S. Tanaka, Nucl. Instrum. Meth. Phys. Res. B 269(14), 1707 (2011).
10. F. Mota, M.-J. Caturla, J.M. Perlado, E. Dominguez, and A. Kubota, J. Nucl. Mater. **329-333(B)**, 1190 (2004).
11. B. Park, W.J. Weber, and L.R. Corrales, Nucl. Instrum. Meth. Phys. Res. B **166-167**, 357 (2000).
12. J.M. Meese and D.R. Locker, Sol. St. Commun. **11**, 1547 (1972).
13. J. Morris, B.J. Cowen, S. Teysseyre, and A.A. Hecht, Comp. Mater. Sci. **109**, 293 (2020).
14. ESTAR: Stopping Power and Range Tables for Electrons, website: https://physics.nist.gov.
15. Screened Relativistic Nuclear Stopping Power: SR-NIEL, website: www.sr-niel org.
16. M.J. Meshishnek, M.R. Ciafolo, and S.H. Liu, *Proton Exposure Testing of Solar Cell Coverglasses*, Los Angeles, CA, USA, Aerospace Corp., 3000 (Dec. 2005).
17. M.J. Meshishnek, W.K. Stuckey, and P.C. Anderson, Radiation Environment Predictions for Laboratory Tests, Los Angeles, Ca, USA, Aerospace Corp., 8565 (Oct. 2001).
18. S.R. Messenger, F. Wong, B. Hoang, C.D. Cress, R.J. Walters, C.A. Kluever, and G. Jones, IEEE Trans. Nucl. Sci. **61**(6), 3348 (2014).